Calculation of the cyclotron-resonance spectrum in the quantum limit for semiconductors (lowest-order Born approximation)

J. Van Royen,* J. De Sitter, and J. T. Devreese†
University of Antwerp (Rijksuniversitair Centrum Antwerpen), Groenenborgerlaan 171, B-2020 Antwerpen, Belgium
(Received 4 August 1983; revised manuscript received 12 June 1984)

Starting from the Kubo formula, the quantum-limit cyclotron-resonance spectrum is calculated for free carriers in a semiconductor. Ionized-impurity and LO-phonon scattering are investigated in the lowest-order Born approximation. For $T>15$ K, excellent agreement is obtained with cyclotron-resonance linewidth measurements of Matsuda *et al.* in InSb. Cyclotron-resonance harmonics and phonon-assisted harmonics are also discussed. No adjustable parameters are introduced.

I. INTRODUCTION

For more than a decade there has been interest in the experimental and theoretical study of the cyclotron-resonance linewidth in semiconductors at low temperatures.[1–36] However, as it has been stated before, "a large number of investigations, both experimental and theoretical, have produced a bewildering variety of (sometimes contradictory) results."[20,34] The situation remains unclear.

The present calculation was stimulated by measurements of Matsuda and Otsuka,[29] who investigated the cyclotron-resonance linewidth in indium antimonide in a temperature range from 4.2 up to 160 K. Earlier measurements in InSb had concentrated on the $T\simeq 4$ K region, where ionized-impurity scattering is considered to be dominant.[7,11,12,18–20] The observations of different groups at this temperature, however, do not agree. It is possible to explain this result by assuming that the effective electron-impurity potential in InSb at $T\simeq 4$ K is strongly dependent on the specific properties of each sample. Theoretically, the problem has been treated by introducing adjustable parameters.[21] For low temperatures, however, there exists no theoretical understanding of the conditions governing the variation of the effective electron-impurity interaction, as a function of different sample properties. For higher temperatures there are reasons to believe that the situation is less complicated: A Debye-screened Coulomb potential is considered to be a reasonable first approximation.[9,37,38]. Yet, as we will illustrate in Sec. V, various sophisticated calculations, all starting from a bare or Debye-screened Coulomb potential, lead to very different results.[2,9,16,17,22,30] This is due to the introduction of a large variety of approximations, the validity of which is difficult to judge. We will also show that the agreement of these calculations with experiment is poor. In view of this situation we have decided to start from an elementary model and to make as simple approximations as possible. A parabolic band electron is considered in a constant external magnetic field. Spin effects are neglected. Electron-electron interaction is not taken into account (low-carrier-concentration limit). No adjustable parameters are introduced. The linear response to an oscillating electric field is calculated from the Kubo formula.[39] In Sec. II the magneto-optical spectrum is obtained in second-order perturbation theory with respect to the scattering potential (lowest-order Born approximation). In Secs. III and IV the resulting formulas are applied to ionized-impurity and longitudinal-optical-phonon scattering, respectively. In Sec. V the calculated linewidths are compared with experiment. Cyclotron-resonance harmonics and phonon-assisted harmonics are also considered. Finally, the validity, limitations, and possible improvements of the calculation are discussed in Sec. VI. A preliminary, partial account of this work has been given in Ref. 40.

II. FREQUENCY-DEPENDENT RESPONSE OF A SCATTERED ELECTRON IN A MAGNETIC FIELD

A. Transformation of the Hamiltonian to a simple form

We consider a parabolic band electron in a constant external magnetic field H along the z axis. In the Landau gauge this field is determined by the vector potential

$$\vec{A}=-Hy\vec{e}_x \ . \tag{2.1}$$

The system under consideration is then described by the Hamiltonian

$$\mathscr{H}=\frac{1}{2m}\left[\vec{p}+\frac{e}{c}\vec{A}\right]^2+H_{\rm sc}+H_{\rm int}$$

$$=H_0+H_{\rm int} \ . \tag{2.2}$$

In Eq. (2.2), m is the parabolic band mass, $-|e|$ is the electron charge, and c is the velocity of light. $H_{\rm sc}$ describes the free scatterers (e.g., phonons, impurities, etc.) and $H_{\rm int}$ is the interaction term. In order to simplify the calculations we perform a canonical transformation introduced by Larsen.[41] Any operator B is transformed to

$$B^{\rm tr}=\exp\left[i\frac{p_xp_y}{m\hbar\omega_c}\right]B\exp\left[-i\frac{p_xp_y}{m\hbar\omega_c}\right], \tag{2.3}$$

where $\hbar$ is Planck's constant and $\omega_c=eH/mc$ is the cyclotron-resonance frequency. Only terms containing x

or y are influenced by this transformation:

$$x^{\rm tr}=x+\frac{1}{m\omega_c}p_y\ , \tag{2.4a}$$

$$y^{\rm tr}=y+\frac{1}{m\omega_c}p_x\ . \tag{2.4b}$$

Introducing the Landau-level raising and lowering operators,

$$b^\dagger=\frac{1}{(2m\hbar\omega_c)^{1/2}}p_x+i\left[\frac{m\omega_c}{2\hbar}\right]^{1/2}y \tag{2.5a}$$

and

$$b=\frac{1}{(2m\hbar\omega_c)^{1/2}}p_y-i\left[\frac{m\omega_c}{2\hbar}\right]^{1/2}y\ , \tag{2.5b}$$

one can rewrite the transformed Hamiltonian as

$$\begin{aligned}\mathscr{H}^{\rm tr}&=\hbar\omega_c(b^\dagger b+\tfrac{1}{2})+\frac{1}{2m}p_z^2+H_{\rm sc}^{\rm tr}+H_{\rm int}^{\rm tr}\\&=H_0^{\rm tr}+H_{\rm int}^{\rm tr}\ .\end{aligned} \tag{2.6}$$

The transverse motion of the unperturbed electron is now described by a simple one-dimensional harmonic oscillator. This will cause a considerable simplification of the following calculations.

B. Kubo formula for a scattered electron in a magnetic field

Consider a conduction electron in an oscillating external electric field. In the weak-field limit the absorption of energy by the electron is adequately described by linear-response theory. Physically relevant quantities, such as the mobility and the optical-absorption coefficient, can be obtained from the conductivity tensor $\overleftrightarrow{\sigma}$. Explicit expressions for the elements of $\overleftrightarrow{\sigma}$ have been formulated in linear-response theory by Kubo.[39] We will now rewrite these expressions in a form well suited for explicit calculations. We start from the expression for the elements of $\overleftrightarrow{\sigma}$, given in Ref. 42, and we consider the $q=0$ limit:

$$\sigma_{uv}=\lim_{\epsilon\to 0}\left[\frac{ne^2i\delta_{u,v}}{m(\omega+i\epsilon)}+\frac{n}{\hbar(\omega+i\epsilon)}\int_{-\infty}^{0}dt\,e^{-i(\omega+i\epsilon)t}\langle[j_u,e^{i\mathscr{H}t/\hbar}j_v e^{-i\mathscr{H}t/\hbar}]\rangle\right]. \tag{2.7}$$

In Eq. (2.7), n is the free-carrier concentration, ω is the frequency of the incident radiation, $\langle\ \rangle$ denotes a thermal average, u and v can have the meaning x, y, or z, $\delta_{u,v}$ is the Kronecker δ function, and the current operator j_u is defined as

$$j_u=e\frac{du}{dt}=\frac{e}{\hbar}i[\mathscr{H},u]\ . \tag{2.8}$$

After the canonical transformation (2.3), one obtains

$$(j_x)^{\rm tr}=ie\left[\frac{\hbar\omega_c}{2m}\right]^{1/2}(b^\dagger-b)\ , \tag{2.9a}$$

$$(j_y)^{\rm tr}=e\left[\frac{\hbar\omega_c}{2m}\right]^{1/2}(b^\dagger+b)\ . \tag{2.9b}$$

Consistent with the usual notation, we now define

$$A(t)=e^{i\mathscr{H}^{\rm tr}t/\hbar}A\,e^{-i\mathscr{H}^{\rm tr}t/\hbar} \tag{2.10}$$

for an arbitrary operator A and arbitrary variable t (real or complex).

In the Faraday configuration the response to circularly polarized radiation (passive or active mode) is determined by $\sigma_{xx}\mp i\sigma_{xy}$. From Eqs. (2.7), (2.9), and (2.10) one obtains the following expression for this quantity, after the canonical transformation (2.3):

$$\sigma_{xx}\mp i\sigma_{xy}=\lim_{\epsilon\to 0}\left[\frac{ne^2i}{m(\omega+i\epsilon)}+\frac{ne^2\omega_c}{m(\omega+i\epsilon)}\int_{-\infty}^{0}dt\,e^{-i(\omega+i\epsilon)t}\left\langle\left[\begin{Bmatrix}b^\dagger\\b\end{Bmatrix},\begin{Bmatrix}b\\b^\dagger\end{Bmatrix}(t)\right]\right\rangle\right]. \tag{2.11}$$

As we are interested in sufficiently high temperatures, we will, from now on, consider single-particle expectation values in the canonical ensemble. Performing a partial integration with respect to t,[43] one obtains, from Eq. (2.11),

$$\sigma_{xx}\mp i\sigma_{xy}=\lim_{\epsilon\to 0}\left[\frac{ne^2i}{m(\omega\pm\omega_c+i\epsilon)}+\frac{ne^2\omega_c}{m\hbar(\omega+i\epsilon)(\omega\pm\omega_c+i\epsilon)}\int_{-\infty}^{0}dt\,e^{-i(\omega+i\epsilon)t}\left\langle\left[\begin{Bmatrix}b^\dagger\\b\end{Bmatrix},\left[H_{\rm int}^{\rm tr},\begin{Bmatrix}b\\b^\dagger\end{Bmatrix}\right](t)\right]\right\rangle\right]. \tag{2.12}$$

Consider the identity (canonical ensemble) for arbitrary operators A and B,

$$\langle[A,B]\rangle\equiv-\int_0^\beta ds\,\langle[\mathscr{H}^{\rm tr},A](-i\hbar s)B\rangle \tag{2.13}$$

in Eq. (2.13), $\beta=1/kT$, where k is Boltzmann's constant and T is the absolute temperature.

Using the identity (2.13) we can now rewrite $\sigma_{xx}\mp i\sigma_{xy}$ as

$$\sigma_{xx}\mp i\sigma_{xy}=\lim_{\epsilon\to 0}\left[\frac{ne^2 i}{m(\omega\pm\omega_c+i\epsilon)}\mp\frac{ne^2\omega_c^2}{m(\omega+i\epsilon)(\omega\pm\omega_c+i\epsilon)}\int_{-\infty}^{0}dt\,e^{-i(\omega+i\epsilon)t}\int_0^\beta ds\left\langle\begin{Bmatrix}b^\dagger\\ b\end{Bmatrix}(-i\hbar s)\left[H_{\rm int}^{\rm tr},\begin{Bmatrix}b\\ b^\dagger\end{Bmatrix}\right](t)\right\rangle\right.$$
$$\left.-\frac{ne^2\omega_c}{m\hbar(\omega+i\epsilon)(\omega\pm\omega_c+i\epsilon)}\int_{-\infty}^{0}dt\,e^{-i(\omega+i\epsilon)t}\int_0^\beta ds\left\langle\left[H_{\rm int}^{\rm tr},\begin{Bmatrix}b^\dagger\\ b\end{Bmatrix}\right](-i\hbar s)\left[H_{\rm int}^{\rm tr},\begin{Bmatrix}b\\ b^\dagger\end{Bmatrix}\right](t)\right\rangle\right]. \quad (2.14)$$

Performing a second partial integration with respect to t, and taking into account the identity

$$\int_0^\beta ds\left\langle\begin{Bmatrix}b^\dagger\\ b\end{Bmatrix}(-i\hbar s)\left[H_{\rm int}^{\rm tr},\begin{Bmatrix}b\\ b^\dagger\end{Bmatrix}\right](0)\right\rangle\equiv 0\,, \quad (2.15)$$

one finally obtains

$$\sigma_{xx}\mp i\sigma_{xy}=\lim_{\epsilon\to 0}\left[\frac{ne^2 i}{m(\omega\pm\omega_c+i\epsilon)}-\frac{ne^2\omega_c}{\hbar m(\omega\pm\omega_c+i\epsilon)^2}\int_{-\infty}^{0}dt\,e^{-i(\omega+i\epsilon)t}\right.$$
$$\left.\times\int_0^\beta ds\left\langle\left[H_{\rm int}^{\rm tr},\begin{Bmatrix}b^\dagger\\ b\end{Bmatrix}\right](-i\hbar s)\left[H_{\rm int}^{\rm tr},\begin{Bmatrix}b\\ b^\dagger\end{Bmatrix}\right](t)\right\rangle\right]. \quad (2.16)$$

Note that this expression is the natural extension, to nonzero magnetic field, of the force-force correlation function introduced (for polaron scattering at weak coupling) in Ref. 43. At first sight, Eq. (2.16) is well suited for perturbation theory with respect to $H_{\rm int}^{\rm tr}$. The first term on the right-hand side (rhs) yields the free-electron result. The second term contains two factors $H_{\rm int}^{\rm tr}$. Therefore, second-order perturbation theory with respect to $H_{\rm int}^{\rm tr}$ becomes trivial. It is sufficient to replace $\mathscr{H}^{\rm tr}$ by $H_0^{\rm tr}$ in all exponents arising in Eq. (2.16). All expectation values can then be calculated using unperturbed wave functions:

$$(\sigma_{xx}\mp i\sigma_{xy})^{(2)}=\lim_{\epsilon\to 0}\left[\frac{ne^2 i}{m(\omega\pm\omega_c+i\epsilon)}\right.$$
$$-\frac{ne^2\omega_c}{\hbar m(\omega\pm\omega_c+i\epsilon)^2}\int_{-\infty}^{0}dt\,e^{-i(\omega+i\epsilon)t}\int_0^\beta ds\frac{1}{{\rm Tr}(e^{-\beta H_0^{\rm tr}})}$$
$$\times{\rm Tr}\left[e^{-\beta H_0^{\rm tr}}e^{H_0^{\rm tr}s}\left[H_{\rm int}^{\rm tr},\begin{Bmatrix}b^\dagger\\ b\end{Bmatrix}\right]e^{-H_0^{\rm tr}s}\right.$$
$$\left.\left.\times\,e^{iH_0^{\rm tr}t/\hbar}\left[H_{\rm int}^{\rm tr},\begin{Bmatrix}b\\ b^\dagger\end{Bmatrix}\right]e^{-iH_0^{\rm tr}t/\hbar}\right]\right]. \quad (2.17)$$

It is easy to see, however, that this straightforward perturbation calculation leads to unphysical results. Indeed, a small perturbation is expected to cause a broadening and a shift of the cyclotron-resonance line. It is immediately clear that such a behavior cannot follow from Eq. (2.17). The calculated spectrum will always contain a δ function at $\omega=\mp\omega_c$. Moreover, there is an additional term diverging as $(\omega\pm\omega_c)^{-2}$. In the next section we will show how to obtain more reasonable results.

C. Introduction of a memory function

From the discussion of Eq. (2.17) it follows that a direct perturbation expansion for $\sigma_{xx}\mp i\sigma_{xy}$ is not satisfactory. More physical results can only be obtained from a theory that introduces a broadening and a shift of the cyclotron-resonance line. Moreover, we want a calculation that is simply related to the perturbation theory of Sec. II B. All these requirements are met by the "memory function approach." In this formalism the response function $(\sigma_{xx}\mp i\sigma_{xy})^{(2)}$ is written in the form

$$(\sigma_{xx}\mp i\sigma_{xy})^{(2)}=\frac{ne^2 i}{m(\omega\pm\omega_c+\Xi_\mp^{(2)}(\omega,\omega_c,T))}\,. \quad (2.18)$$

Here, $\Xi_\mp^{(2)}(\omega,\omega_c,T)$ is called the memory function. It is straightforward to write a perturbation expansion for the left-

hand side (lhs) of Eq. (2.18), considering $\Xi_{\mp}^{(2)}(\omega,\omega_c,T)$ as a small quantity. It is then clear that Eqs. (2.17) and (2.18) are equivalent up to second-order perturbation theory with respect to the interaction, provided the memory function $\Xi_{\mp}^{(2)}(\omega,\omega_c,T)$ is given by

$$\Xi_{\mp}^{(2)}(\omega,\omega_c,T)=-i\frac{\omega_c}{\hbar}\lim_{\epsilon\to 0}\int_{-\infty}^{0}dt\,e^{-i(\omega+i\epsilon)t}\int_0^{\beta}ds\frac{1}{\mathrm{Tr}(e^{-\beta H_0^{\mathrm{tr}}})}\mathrm{Tr}\left[e^{-\beta H_0^{\mathrm{tr}}}e^{H_0^{\mathrm{tr}}s}\left[H_{\mathrm{int}}^{\mathrm{tr}},\begin{Bmatrix}b^{\dagger}\\ b\end{Bmatrix}\right]e^{-H_0^{\mathrm{tr}}s}\right.$$
$$\left.\times e^{iH_0^{\mathrm{tr}}t/\hbar}\left[H_{\mathrm{int}}^{\mathrm{tr}},\begin{Bmatrix}b\\ b^{\dagger}\end{Bmatrix}\right]e^{-iH_0^{\mathrm{tr}}t/\hbar}\right]. \tag{2.19}$$

The absorption coefficient for circularly polarized radiation in the Faraday configuration (passive or active mode) is proportional to the real part of $\sigma_{xx}\mp i\sigma_{xy}$. One obtains

$$\mathrm{Re}(\sigma_{xx}\mp i\sigma_{xy})^{(2)}=\frac{ne^2}{m}\frac{\mathrm{Im}\Xi_{\mp}^{(2)}(\omega,\omega_c,T)}{[\omega\pm\omega_c+\mathrm{Re}\Xi_{\mp}^{(2)}(\omega,\omega_c,T)]^2+[\mathrm{Im}\Xi_{\mp}^{(2)}(\omega,\omega_c,T)]^2}\,. \tag{2.20}$$

Although Eqs. (2.17) and (2.18) are equivalent up to second-order perturbation theory with respect to $H_{\mathrm{int}}^{\mathrm{tr}}$, it is intuitively clear that Eqs. (2.18)—(2.20) will lead to more reasonable results. Indeed, for slowly changing $\mathrm{Re}\Xi_{\mp}^{(2)}$ and $\mathrm{Im}\Xi_{\mp}^{(2)}$, it follows from Eq. (2.20) that a quasi-Lorentzian line shape is obtained. The position of the cyclotron-resonance line is then determined by the equation

$$\omega\pm\omega_c+\mathrm{Re}\Xi_{\mp}^{(2)}(\omega,\omega_c,T)=0\,,$$

and the half width is given by

$$\mathrm{Im}\Xi_{\mp}^{(2)}(\omega,\omega_c,T)$$

at the peak maximum.

A further justification for the present approach is given by the zero-magnetic-field case. In Ref. 44 the free-polaron optical absorption was investigated and excellent results were obtained. The present method is a straightforward extension, to include arbitrary magnetic field, of this free-polaron calculation. (For nonzero magnetic field, a similar method has been used in Refs. 7, 23—25, 27, 28, and 33.)

Expression (2.19) will be worked out explicitly in Secs. III and IV for scattering by longitudinal-optical (LO) phonons and ionized impurities. The results will be compared with experiment in Sec. V. The validity of the method, and possible improvements, will be discussed in Sec. VI.

III. LO-PHONON SCATTERING

In polar semiconductors the electron—LO-phonon interaction can be described by the Fröhlich polaron Hamiltonian.[45,46] For this model, one obtains, after the canonical transformation (2.3),

$$H_0^{\mathrm{tr}}=\hbar\omega_c(b^{\dagger}b+\tfrac{1}{2})+\frac{1}{2m}p_z^2+\sum_{\vec{k}}\hbar\omega_{\mathrm{LO}}a_{\vec{k}}^{\dagger}a_{\vec{k}}\,, \tag{3.1}$$

and

$$H_{\mathrm{int}}^{\mathrm{tr}}=\sum_{\vec{k}}\left[V_k a_{\vec{k}}\exp\left\{i\left[k_x x+\frac{k_y p_x}{m\omega_c}+k_z z+(k_x+ik_y)\left[\frac{\hbar}{2m\omega_c}\right]^{1/2}b+(k_x-ik_y)\left[\frac{\hbar}{2m\omega_c}\right]^{1/2}b^{\dagger}\right]\right\}\right]+\mathrm{H.c.} \tag{3.2}$$

In Eqs. (3.1) and (3.2), ω_{LO} is the longitudinal-optical-phonon frequency, and $a_{\vec{k}}^{\dagger}$ and $a_{\vec{k}}$ are the creation and annihilation operators for phonons with wave vector $\vec{k}$; furthermore,

$$V_k=\frac{1}{k}\left[\frac{4\pi}{V}\right]^{1/2}\hbar\omega_{\mathrm{LO}}\left[\frac{\hbar}{2m\omega_{\mathrm{LO}}}\right]^{1/4}\alpha^{1/2}\,. \tag{3.3}$$

In this expression, V is the volume of the crystal and α is the dimensionless Fröhlich coupling constant.

In order to obtain explicit results for the memory function, $\Xi_{\mathrm{pol},\mp}^{(2)}(\omega,\omega_c,T)$, one needs the zeroth-order time dependence of the different operators involved. This is given by

$$a_{\vec{k}}(t)=a_{\vec{k}}\exp(-i\omega_{\mathrm{LO}}t)\,, \tag{3.4a}$$

$$a_{\vec{k}}^{\dagger}(t)=a_{\vec{k}}^{\dagger}\exp(i\omega_{\mathrm{LO}}t)\,, \tag{3.4b}$$

$$b(t)=b\exp(-i\omega_c t)\,, \tag{3.4c}$$

$$b^{\dagger}(t)=b^{\dagger}\exp(i\omega_c t)\,, \tag{3.4d}$$

$$p_x(t)=p_x(0)\,, \tag{3.4e}$$

$$x(t)=x(0)\,, \tag{3.4f}$$

$$p_z(t)=p_z(0)\,, \tag{3.4g}$$

$$z(t)=z(0)+\frac{p_z(0)}{m}t\,. \tag{3.4h}$$

Analogous expressions can be written for the s dependence. Now remember the following operator properties: If the commutator of A and B commutes with A and B, then

$$[A,\exp B]=[A,B]\exp B \tag{3.5}$$

and

$$\exp(A+B)=\exp A\exp B\exp(-\tfrac{1}{2}[A,B])\ . \tag{3.6}$$

The commutators $[H_{\rm int}^{\rm tr},b^\dagger](t)$ and $[H_{\rm int}^{\rm tr},b](-i\hbar s)$ can then be written, in zeroth order, as

$$\begin{aligned}
e^{iH_0^{\rm tr}t/\hbar}[H_{\rm int}^{\rm tr},b^\dagger]e^{-iH_0^{\rm tr}t/\hbar}=&\sum_{\vec{k}}\sum_{n_1,n_2=0}^{\infty} i(k_x+ik_y)\left[\frac{\hbar}{2m\omega_c}\right]^{1/2}V_k a_{\vec{k}}e^{-i\omega_{\rm LO}t}\exp\left[i\left[k_x x+\frac{k_y p_x}{m\omega_c}+k_z z\right]\right]\\
&\times\exp\left[-\frac{\hbar(k_x^2+k_y^2)}{4m\omega_c}\right]\exp\left[i\frac{k_z p_z}{m}t\right]\exp\left[i\frac{\hbar k_z^2}{2m}t\right]\frac{(i)^{n_1+n_2}(k_x-ik_y)^{n_1}(k_x+ik_y)^{n_2}}{n_1!n_2!}\\
&\times\left[\frac{\hbar}{2m\omega_c}\right]^{(n_1+n_2)/2}(b^\dagger)^{n_1}(b)^{n_2}e^{i(n_1-n_2)\omega_c t}\\
-\sum_{\vec{k}}\sum_{n_3,n_4=0}^{\infty}&i(k_x+ik_y)\left[\frac{\hbar}{2m\omega_c}\right]^{1/2}V_k a_{\vec{k}}^\dagger e^{i\omega_{\rm LO}t}\exp\left[-i\left[k_x x+\frac{k_y p_x}{m\omega_c}+k_z z\right]\right]\\
&\times\exp\left[-\frac{\hbar(k_x^2+k_y^2)}{4m\omega_c}\right]\exp\left[-i\frac{k_z p_z}{m}t\right]\\
&\times\exp\left[i\frac{\hbar k_z^2}{2m}t\right]\frac{(-i)^{n_3+n_4}(k_x-ik_y)^{n_3}(k_x+ik_y)^{n_4}}{n_3!n_4!}\\
&\times\left[\frac{\hbar}{2m\omega_c}\right]^{(n_3+n_4)/2}(b^\dagger)^{n_3}(b)^{n_4}e^{i(n_3-n_4)\omega_c t}
\end{aligned}\tag{3.7}$$

and

$$\begin{aligned}
e^{H_0^{\rm tr}s}[H_{\rm int}^{\rm tr},b]e^{-H_0^{\rm tr}s}=&-\sum_{\vec{k}}\sum_{m_1,m_2=0}^{\infty} i(k_x-ik_y)\left[\frac{\hbar}{2m\omega_c}\right]^{1/2}V_k a_{\vec{k}}e^{-\hbar\omega_{\rm LO}s}\exp\left[\hbar\frac{k_z p_z}{m}s\right]\\
&\times\exp\left[i\left[k_x x+\frac{k_y p_x}{m\omega_c}+k_z z\right]\right]\exp\left[-\frac{\hbar(k_x^2+k_y^2)}{4m\omega_c}\right]\\
&\times\exp\left[-\frac{\hbar^2 k_z^2}{2m}s\right]\frac{(i)^{m_1+m_2}(k_x-ik_y)^{m_1}(k_x+ik_y)^{m_2}}{m_1!m_2!}\\
&\times\left[\frac{\hbar}{2m\omega_c}\right]^{(m_1+m_2)/2}(b^\dagger)^{m_1}(b)^{m_2}e^{(m_1-m_2)\hbar\omega_c s}\\
+\sum_{\vec{k}}\sum_{m_3,m_4=0}^{\infty}&i(k_x-ik_y)V_k a_{\vec{k}}^\dagger e^{\hbar\omega_{\rm LO}s}\exp\left[-\hbar\frac{k_z p_z}{m}s\right]\\
&\times\exp\left[-i\left[k_x x+\frac{k_y p_x}{m\omega_c}+k_z z\right]\right]\exp\left[-\frac{\hbar(k_x^2+k_y^2)}{4m\omega_c}\right]\\
&\times\exp\left[-\frac{\hbar^2 k_z^2}{2m}s\right]\frac{(-i)^{m_3+m_4}(k_x-ik_y)^{m_3}(k_x+ik_y)^{m_4}}{m_3!m_4!}\\
&\times\left[\frac{\hbar}{2m\omega_c}\right]^{(m_3+m_4)/2}(b^\dagger)^{m_3}(b)^{m_4}e^{(m_3-m_4)\hbar\omega_c s}\ .
\end{aligned}\tag{3.8}$$

In the canonical ensemble, the expectation value of an arbitrary operator A is given by

$$\langle A\rangle=\frac{\prod_{\vec{k}}\sum_{n_{\vec{k}}=0}^{\infty}\sum_{N=0}^{\infty}\int_{-\infty}^{+\infty}dp_z e^{-\beta n_{\vec{k}}\hbar\omega_{\mathrm{LO}}}e^{-\beta N\hbar\omega_c}e^{-\beta(p_z^2/2m)}\langle n_{\vec{k}}|\langle N|\langle p_z|A|p_z\rangle|N\rangle|n_{\vec{k}}\rangle}{\prod_{\vec{k}}\sum_{n_{\vec{k}}=0}^{\infty}\sum_{N=0}^{\infty}\int_{-\infty}^{+\infty}dp_z e^{-\beta n_{\vec{k}}\hbar\omega_{\mathrm{LO}}}e^{-\beta N\hbar\omega_c}e^{-\beta(p_z^2/2m)}}\ . \tag{3.9}$$

Note that Eq. (3.9) takes into account the population of the higher Landau levels as temperature is raised.

Substituting Eqs. (3.7) and (3.8) into Eq. (2.19), and applying Eq. (3.9), one obtains $\Xi^{(2)}_{\mathrm{pol},\mp}(\omega,\omega_c,T)$ for Fröhlich polarons, in the lowest-order Born approximation. After a lengthy, but straightforward calculation, one finds, for the imaginary part of the memory function,

$$\begin{aligned}\mathrm{Im}\Xi^{(2)}_{\mathrm{pol},\perp}(\omega,\omega_c,T)=&\frac{\alpha\omega_c\omega_{\mathrm{LO}}(\beta\hbar\omega_{\mathrm{LO}})^{1/2}(1-e^{-\beta\hbar\omega_c})\sinh(\beta\hbar\omega/2)}{2\omega\sqrt{\pi}\sinh(\beta\hbar\omega_{\mathrm{LO}}/2)}\\&\times\sum_{N=0}^{\infty}\sum_{m_1=0}^{N}\sum_{m_2=0}^{\infty}\sum_{n_1=0}^{\infty}\sum_{n_2=0}^{N}\\&\times\frac{(-1)^{m_1-n_2}\exp\left[-\beta\hbar\omega_c\left[N+\frac{n_1-n_2}{2}\right]\right]N!(N-n_2+n_1)!(m_1+n_1)!\delta_{(n_1-n_2),(m_2-m_1)}}{m_1!m_2!n_1!n_2!(N-m_1)!(N-n_2)!}\\&\times(T_1+T_2+T_3+T_4)\ .\end{aligned} \tag{3.10a}$$

In this expression, the terms T_1, T_2, T_3, and T_4 are defined as follows:

$$T_1=K_0(\tfrac{1}{2}\beta\hbar\,|\,\omega-\omega_{\mathrm{LO}}+(m_1-m_2)\omega_c\,|\,)\ , \tag{3.10b}$$

$$T_2=K_0(\tfrac{1}{2}\beta\hbar\,|\,\omega+\omega_{\mathrm{LO}}-(m_1-m_2)\omega_c\,|\,)\ , \tag{3.10c}$$

$$T_3=-\frac{1}{2}\frac{\omega_{\mathrm{LO}}}{\omega_c}\int_0^{\infty}dx\exp\left[\frac{-\beta\hbar[\omega-\omega_{\mathrm{LO}}-(n_1-n_2)\omega_c]^2}{4\omega_{\mathrm{LO}}x}-\frac{\beta\hbar\omega_{\mathrm{LO}}x}{4}-\frac{\omega_{\mathrm{LO}}x}{\omega_c}\right]E_{m_1+n_1+1}\left[\frac{\omega_{\mathrm{LO}}x}{\omega_c}\right]\ , \tag{3.10d}$$

$$T_4=-\frac{1}{2}\frac{\omega_{\mathrm{LO}}}{\omega_c}\int_0^{\infty}dx\exp\left[\frac{-\beta\hbar[\omega+\omega_{\mathrm{LO}}+(n_1-n_2)\omega_c]^2}{4\omega_{\mathrm{LO}}x}-\frac{\beta\hbar\omega_{\mathrm{LO}}x}{4}-\frac{\omega_{\mathrm{LO}}x}{\omega_c}\right]E_{m_1+n_1+1}\left[\frac{\omega_{\mathrm{LO}}x}{\omega_c}\right]\ , \tag{3.10e}$$

The real part of the memory function is obtained as

$$\begin{aligned}\mathrm{Re}\Xi^{(2)}_{\mathrm{pol},\perp}(\omega,\omega_c,T)=&\frac{\alpha\omega_c\omega_{\mathrm{LO}}(\beta\hbar\omega_{\mathrm{LO}})^{1/2}(1-e^{-\beta\hbar\omega_c})}{2\omega\sqrt{\pi}\sinh(\beta\hbar\omega_{\mathrm{LO}}/2)}\\&\times\sum_{N=0}^{\infty}\sum_{m_1=0}^{N}\sum_{m_2=0}^{\infty}\sum_{n_1=0}^{\infty}\sum_{n_2=0}^{N}\\&\times\frac{(-1)^{m_1-n_2}\exp\left[-\beta\hbar\omega_c\left[N+\frac{n_1-n_2}{2}\right]\right]N!(N-n_2+n_1)!(m_1+n_1)!\delta_{(n_1-n_2),(m_2-m_1)}}{m_1!m_2!n_1!n_2!(N-m_1)!(N-n_2)!}\\&\times\left[W_1+W_2+W_3+W_4+W_5+\frac{\omega_{\mathrm{LO}}}{4\omega_c\sqrt{\pi}}\int_{-\infty}^{+\infty}du\,u\exp\left[\frac{u^2\omega_{\mathrm{LO}}}{2\omega_c}\right]E_{m_1+n_1+1}\left[\frac{u^2\omega_{\mathrm{LO}}}{2\omega_c}\right]\right.\\&\left.\times(V_1+V_2+V_3+V_4+V_5+V_6)\right]\ .\end{aligned} \tag{3.10f}$$

In this expression, the terms W_1,W_2,W_3,W_4,W_5 and V_1,V_2,V_3,V_4,V_5,V_6 are defined, respectively, as

$$W_1=-\pi I_0(\tfrac{1}{2}\beta\hbar[\omega_{\rm LO}+(n_1-n_2)\omega_c])\ , \tag{3.10g}$$

$$W_2=\frac{\pi}{2}e^{\beta(\hbar\omega/2)}I_0(\tfrac{1}{2}\beta\hbar[-\omega+\omega_{\rm LO}+(n_1-n_2)\omega_c])\Theta(-\omega+\omega_{\rm LO}+(n_1-n_2)\omega_c)\ , \tag{3.10h}$$

$$W_3=\frac{\pi}{2}e^{-\beta(\hbar\omega/2)}I_0(\tfrac{1}{2}\beta\hbar[\omega+\omega_{\rm LO}+(n_1-n_2)\omega_c])\Theta(\omega+\omega_{\rm LO}+(n_1-n_2)\omega_c)\ , \tag{3.10i}$$

$$W_4=\frac{\pi}{2}e^{-\beta(\hbar\omega/2)}I_0(\tfrac{1}{2}\beta\hbar[\omega-\omega_{\rm LO}+(n_1-n_2)\omega_c])\Theta(\omega-\omega_{\rm LO}+(n_1-n_2)\omega_c)\ , \tag{3.10j}$$

$$W_5=\frac{\pi}{2}e^{\beta(\hbar\omega/2)}I_0(\tfrac{1}{2}\beta\hbar[-\omega-\omega_{\rm LO}+(n_1-n_2)\omega_c])\Theta(-\omega-\omega_{\rm LO}+(n_1-n_2)\omega_c)\ , \tag{3.10k}$$

$$V_1=2\exp\{\tfrac{1}{2}\beta\hbar[\omega_{\rm LO}+(m_2-m_1)\omega_c]\}D\left[\left[\frac{\beta\hbar\omega_{\rm LO}}{2}\right]^{1/2}\left[\frac{u}{2}+\frac{\omega_{\rm LO}+(m_2-m_1)\omega_c}{u\omega_{\rm LO}}\right]\right]\ , \tag{3.10l}$$

$$V_2=2\exp\{\tfrac{1}{2}\beta\hbar[-\omega_{\rm LO}+(m_2-m_1)\omega_c]\}D\left[\left[\frac{\beta\hbar\omega_{\rm LO}}{2}\right]^{1/2}\left[\frac{u}{2}+\frac{-\omega_{\rm LO}+(m_2-m_1)\omega_c}{u\omega_{\rm LO}}\right]\right]\ , \tag{3.10m}$$

$$V_3=-\exp\{\tfrac{1}{2}\beta\hbar[\omega_{\rm LO}+(m_2-m_1)\omega_c]\}D\left[\left[\frac{\beta\hbar\omega_{\rm LO}}{2}\right]^{1/2}\left[\frac{u}{2}+\frac{\omega_{\rm LO}+(m_2-m_1)\omega_c}{u\omega_{\rm LO}}\right]\right]\ , \tag{3.10n}$$

$$V_4=-\exp\{\tfrac{1}{2}\beta\hbar[-\omega_{\rm LO}+(m_2-m_1)\omega_c]\}D\left[\left[\frac{\beta\hbar\omega_{\rm LO}}{2}\right]^{1/2}\left[\frac{u}{2}+\frac{-\omega_{\rm LO}+(m_2-m_1)\omega_c+\omega}{u\omega_{\rm LO}}\right]\right]\ , \tag{3.10o}$$

$$V_5=-\exp\{\tfrac{1}{2}\beta\hbar[-\omega_{\rm LO}+(m_2-m_1)\omega_c]\}D\left[\left[\frac{\beta\hbar\omega_{\rm LO}}{2}\right]^{1/2}\left[\frac{u}{2}+\frac{-\omega_{\rm LO}+(m_2-m_1)\omega_c-\omega}{u\omega_{\rm LO}}\right]\right]\ , \tag{3.10p}$$

$$V_6=-\exp\{\tfrac{1}{2}\beta\hbar[\omega_{\rm LO}+(m_2-m_1)\omega_c]\}D\left[\left[\frac{\beta\hbar\omega_{\rm LO}}{2}\right]^{1/2}\left[\frac{u}{2}+\frac{\omega_{\rm LO}+(m_2-m_1)\omega_c+\omega}{u\omega_{\rm LO}}\right]\right]\ . \tag{3.10q}$$

Note that $\Xi^{(2)}_{\rm pol,-}(\omega,\omega_c,T)=\Xi^{(2)}_{\rm pol,+}(\omega,\omega_c,T)$. Therefore the simplified notation $\Xi^{(2)}_{\rm pol,\perp}(\omega,\omega_c,T)$ is introduced. In Eqs. (3.10), $\Theta(x)$ is the Heaviside step function: $\Theta(x)=0$ for $x\le 0$; $\Theta(x)=1$ for $x>0$. We write

$$K_0\left[\frac{|a|}{2}\right]=e^{-|a|/2}\int_0^\infty\frac{du\,e^{-u}}{\sqrt{u(u+|a|)}}\quad\text{and}\quad I_0\left[\frac{a}{2}\right]=\frac{1}{\pi}\exp\left[\frac{a}{2}\right]\int_0^\infty\frac{du\,e^{-u}}{\sqrt{u(u-x)}}\ ,$$

which are Bessel functions of the second kind (Ref. 47, Secs. 3.364.1 and 3.364.3). $D(x)$ is Dawson's integral (Ref. 48, Secs. 7.1.3, 7.1.4, and 7.1.16); $E_n(x)$ is the exponential integral function of order n (Ref. 48, Sec. 5.1.4; Ref. 47, Sec. 8.353.3). In the derivation of Eqs. (3.10), use has been made of the well-known representation

$$\lim_{\epsilon\to 0}\int_{-\infty}^{0}dt\,e^{-i(x+i\epsilon)t}=\pi\delta(x)+i\,{\rm P}(1/x)\ , \tag{3.11}$$

where P indicates the principal value. Moreover, the summation over $\vec{\rm k}$ space has been converted into an integral via

$$\sum_{\vec{\rm k}}f(\vec{\rm k})=\frac{V}{(2\pi)^3}\int_V d\vec{\rm k}\,f(\vec{\rm k})\ . \tag{3.12}$$

Finally, use has been made of the following transformation:

$$\sum_{N=0}^{\infty}\sum_{m_1=0}^{N}\sum_{m_2=0}^{\infty}\sum_{n_1=0}^{\infty}\sum_{n_2=0}^{N}f(m_1,m_2,n_1,n_2,N)\delta_{(n_1-n_2),(m_2-m_1)}$$
$$=\sum_{N'=0}^{\infty}\sum_{m_1'=0}^{N'}\sum_{m_2'=0}^{\infty}\sum_{n_1'=0}^{\infty}\sum_{n_2'=0}^{N'}f(m_2',m_1',n_2',n_1',N'+n_1'-n_2')\delta_{(n_1'-n_2'),(m_2'-m_1')}\ . \tag{3.13}$$

In this equation, $f(m_1,m_2,n_1,n_2,N)$ is an arbitrary function, and the new summation indices are defined as follows:

$$N'=N-n_2+n_1 , \tag{3.14a}$$

$$m_1'=m_2 , \tag{3.14b}$$

$$m_2'=m_1 , \tag{3.14c}$$

$$n_1'=n_2 , \tag{3.14d}$$

$$n_2'=n_1 . \tag{3.14e}$$

As a result of this transformation one has immediately, from Eqs. (3.10), the following symmetry relations:

$$\mathrm{Im}\Xi^{(2)}_{\mathrm{pol},\perp}(-\omega,\omega_c,T)=\mathrm{Im}\Xi^{(2)}_{\mathrm{pol},\perp}(\omega,\omega_c,T) , \tag{3.15a}$$

$$\mathrm{Re}\Xi^{(2)}_{\mathrm{pol},\perp}(-\omega,\omega_c,T)=-\mathrm{Re}\Xi^{(2)}_{\mathrm{pol},\perp}(\omega,\omega_c,T) . \tag{3.15b}$$

The imaginary part of $\Xi^{(2)}_{\mathrm{pol},\perp}$ is an even function of ω, and the real part is an odd function of ω. The results of Eqs. (3.10) have been evaluated numerically. In Fig. 1 typical plots of $\mathrm{Im}\Xi^{(2)}_{\mathrm{pol},\perp}$, $\mathrm{Re}\Xi^{(2)}_{\mathrm{pol},\perp}$, and $\mathrm{Re}(\sigma_{xx}+i\sigma_{xy})^{(2)}_{\mathrm{pol}}$ are shown, as a function of $\omega/\omega_{\mathrm{LO}}$. The imaginary part of $\Xi^{(2)}_{\mathrm{pol},\perp}$ exhibits logarithmic divergences for $\omega=\omega_{\mathrm{LO}}\pm n\omega_c$ and $\omega=-\omega_{\mathrm{LO}}\pm n\omega_c$. Associated with these divergences, the real part shows finite, discontinuous jumps. In the absorption coefficient, the singularities give rise to the well-known phonon-assisted cyclotron-resonance harmonics.[49–52] These peaks correspond to simple physical processes: The electron, stimulated by the radiation, is moved up or down n Landau levels, and simultaneously a phonon is emitted or absorbed. The divergent behavior of the present calculation is a consequence of the use of second-order perturbation theory (lowest-order Born approximation). It is related to the inverse-square-root divergence of the unperturbed density of states for the z direction. In a more sophisticated theory, the divergences will be finite maxima, and the jumps will become continuous.

For $\omega\simeq\omega_c$ the cyclotron-resonance peak is observed. It is clear that, for $\omega_c\gg\omega_{\mathrm{LO}}$ or $\omega_c\ll\omega_{\mathrm{LO}}$, its position is determined by the equation

$$\omega-\omega_c+\mathrm{Re}\Xi^{(2)}_{\mathrm{pol},\perp}(\omega,\omega_c,T)=0 , \tag{3.16}$$

and its width is given by $\mathrm{Im}\Xi^{(2)}_{\mathrm{pol},\perp}(\omega,\omega_c,T)$ at the maximum.

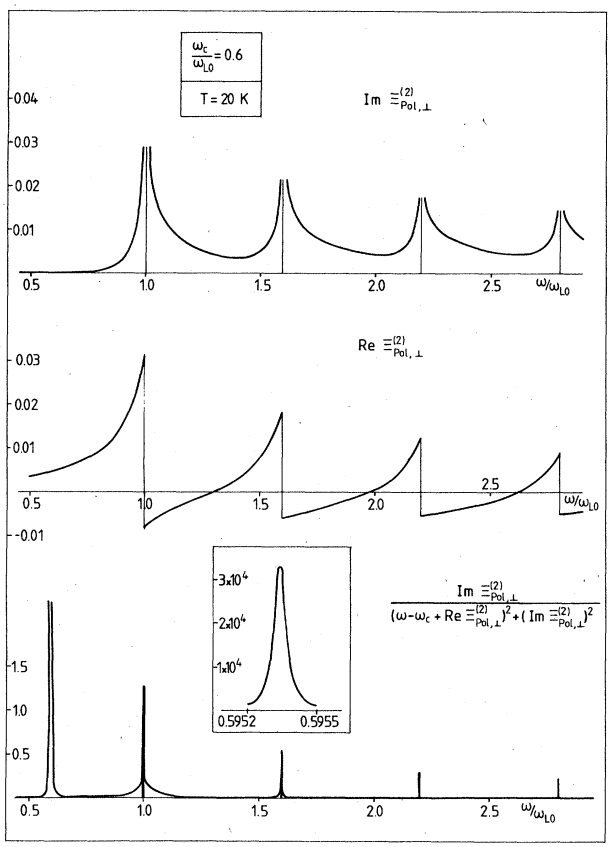

FIG. 1. Typical numerical results for the polaron magneto-optical response functions in the Faraday configuration. The following parameters have been used: polaron coupling constant, $\alpha=0.02$; LO-phonon energy, $\hbar\omega_{\mathrm{LO}}=24.4$ meV; parabolic band mass, $m=0.0139m_0$; cyclotron-resonance frequency, $\omega_c=0.6\omega_{\mathrm{LO}}$; temperature, $T=20$ K. The real and imaginary parts of the memory function $\Xi^{(2)}_{\mathrm{pol},\perp}$ are calculated using Eqs. (3.10a) and (3.10b). The imaginary part of $\Xi^{(2)}_{\mathrm{pol},\perp}$ shows logarithmic divergences at $\omega=\omega_{\mathrm{LO}}+n\omega_c$. The real part shows finite jumps at the same frequencies. The absorption spectrum in the active mode is calculated using Eq. (2.20). The cyclotron-resonance peak at $\omega\simeq0.6\omega_{\mathrm{LO}}$ is slightly shifted and broadened. In the inset it is shown completely, using different scales. At $\omega=\omega_{\mathrm{LO}}$ the one-phonon peak is observed. Phonon-assisted harmonics occur at $\omega/\omega_{\mathrm{LO}}=1.6, 2.2, 2.8, \ldots$. The response functions, which have dimension s, are given in units where $\omega_{\mathrm{LO}}=1$.

IV. IONIZED-IMPURITY SCATTERING

In this section we consider elastic scattering of the charge carriers by ionized impurities. In a typical semiconductor the mass of the impurity is several orders of magnitude larger than the electron effective mass. Therefore it is a reasonable approximation to take the mass of the impurity to be infinite in the present calculation. After the canonical transformation (2.3), one then obtains the following unperturbed Hamiltonian:

$$H_0^{\mathrm{tr}}=\hbar\omega_c(b^\dagger b+\tfrac{1}{2})+\frac{1}{2m}p_z^2 . \tag{4.1}$$

A long-standing problem is the form of the interaction potential between the electron and the ionized impurities. Although much work has been done on this subject, the situation is quite unclear, especially in the lower-temperature region ($T\lesssim4$ K in InSb). Several potentials, with different screening, have been proposed.[8–10,21,37,38,53] In the present work, however, our comparisons will be made with experiments at somewhat higher temperatures. In that case, a Debye-screened Coulomb potential is believed to be a reasonable approximation,[9,37,38]

$$H_{\mathrm{int}}=-\frac{e^2}{\kappa}\sum_{j=1}^{\mathcal{N}}\frac{\exp(-|\vec{r}-\vec{R}_j|/L_D)}{|\vec{r}-\vec{R}_j|} . \tag{4.2}$$

The Debye-screening length L_D is given by

$$L_D=\left[\frac{\kappa kT}{4\pi ne^2}\right]^{1/2}. \tag{4.3}$$

In Eqs. (4.2) and (4.3), $\mathcal{N}$ is the total number of ionized impurities in the crystal, $\vec{R}_j$ is the position vector of the jth impurity, and κ is the static dielectric constant of the medium; n is the free-carrier concentration.

After the canonical transformation (2.3), the interaction term can be rewritten as

$$H_{\rm int}^{\rm tr}=\sum_{j=1}^{\mathcal{N}}\sum_{\vec{k}} W_k \exp\left\{i\left[-\vec{k}\cdot\vec{R}_j+k_x x+\frac{k_y p_x}{m\omega_c}+k_z z+(k_x+ik_y)\left[\frac{\hbar}{2m\omega_c}\right]^{1/2} b+(k_x-ik_y)\left[\frac{\hbar}{2m\omega_c}\right]^{1/2} b^\dagger\right]\right\}. \tag{4.4}$$

In this expression, the Fourier component W_k is given by

$$W_k=-\frac{4\pi e^2}{V\kappa}\frac{1}{k^2+L_D^{-2}}. \tag{4.5}$$

The memory function $\Xi^{(2)}_{{\rm imp},\mp}(\omega,\omega_c,T)$ for ionized-impurity scattering can then be calculated, in second-order perturbation theory with respect to $H_{\rm int}^{\rm tr}$. Again, we start from Eq. (2.19). The commutators $[H_{\rm int}^{\rm tr},b^\dagger](t)$ and $[H_{\rm int}^{\rm tr},b](-i\hbar s)$ can now be rewritten, in zeroth order, as

$$\begin{aligned}e^{iH_0t/\hbar}[H_{\rm int}^{\rm tr},b^\dagger]e^{-iH_0t/\hbar}=&\sum_{j=1}^{\mathcal{N}}\sum_{\vec{k}}\sum_{n_1,n_2=0}^{\infty} i(k_x+ik_y)\left[\frac{\hbar}{2m\omega_c}\right]^{1/2} W_k e^{-i\vec{k}\cdot\vec{R}_j}\exp\left[i\left[k_x x+\frac{k_y p_x}{m\omega_c}+k_z z\right]\right]\\ &\times\exp\left[-\frac{\hbar(k_x^2+k_y^2)}{4m\omega_c}\right]\exp\left[i\frac{k_z p_z}{m}t\right]\exp\left[i\frac{\hbar k_z^2}{2m}t\right]\frac{(i)^{n_1+n_2}(k_x-ik_y)^{n_1}(k_x+ik_y)^{n_2}}{n_1!n_2!}\\ &\times\left[\frac{\hbar}{2m\omega_c}\right]^{(n_1+n_2)/2}(b^\dagger)^{n_1}(b)^{n_2}e^{i(n_1-n_2)\omega_c t}\end{aligned} \tag{4.6}$$

and

$$\begin{aligned}e^{H_0s}[H_{\rm int}^{\rm tr},b]e^{-H_0s}=&-\sum_{j=1}^{\mathcal{N}}\sum_{\vec{k}}\sum_{m_1,m_2=0}^{\infty} i(k_x-ik_y)\left[\frac{\hbar}{2m\omega_c}\right]^{1/2} W_k e^{i\vec{k}\cdot\vec{R}_j}\exp\left[\hbar\frac{k_z p_z}{m}s\right]\\ &\times\exp\left[i\left[k_x x+\frac{k_y p_x}{m\omega_c}+k_z z\right]\right]\\ &\times\exp\left[-\frac{\hbar(k_x^2+k_y^2)}{4m\omega_c}\right]\exp\left[-\frac{\hbar^2k_z^2}{2m}s\right]\frac{(i)^{m_1+m_2}(k_x-ik_y)^{m_1}(k_x+ik_y)^{m_2}}{m_1!m_2!}\\ &\times\left[\frac{\hbar}{2m\omega_c}\right]^{(m_1+m_2)/2}(b^\dagger)^{m_1}(b)^{m_2}e^{(m_1-m_2)\hbar\omega_c s}.\end{aligned} \tag{4.7}$$

Substituting Eqs. (4.6) and (4.7) into Eq. (2.19), one obtains $\Xi^{(2)}_{{\rm imp},\mp}(\omega,\omega_c,T)$ for ionized-impurity scattering in the lowest-order Born approximation. In the explicit calculation, only single-site-scattering events have been taken into account (low-impurity-concentration limit). After a long, but straightforward calculation one finds

$$\begin{aligned}{\rm Im}\Xi^{(2)}_{{\rm imp},\perp}(\omega,\omega_c,T)=&\frac{2n_I(2\pi\beta)^{1/2}e^4(1-e^{-\beta\hbar\omega_c})\sinh(\beta\hbar\omega/2)}{m^{1/2}\kappa^2\hbar\omega}\\ &\times\sum_{N=0}^{\infty}\sum_{m_1=0}^{N}\sum_{m_2=0}^{\infty}\sum_{n_1=0}^{\infty}\sum_{n_2=0}^{N}\\ &\times\frac{(-1)^{m_1-n_2}\exp\left[-\beta\hbar\omega_c\left[N+\frac{n_1-n_2}{2}\right]\right]N!(N-n_2+n_1)!(m_1+n_1)!\delta_{(n_1-n_2),(m_2-m_1)}}{m_1!m_2!n_1!n_2!(N-n_2)!(N-m_1)!}\\ &\times\int_0^\infty\frac{dt}{t}\exp\left[-t^2-\frac{\beta^2\hbar^2[\omega-(n_1-n_2)\omega_c]^2}{16t^2}\right][-1+(x+m_1+n_1+1)e^x E_{m_1+n_1+1}(x)]\end{aligned} \tag{4.8a}$$

and

$$\mathrm{Re}\Xi^{(2)}_{\mathrm{imp},\perp}(\omega,\omega_c,T)=\frac{2n_I(2\beta)^{1/2}e^4(1-e^{-\beta\hbar\omega_c})}{m^{1/2}\kappa^2\hbar\omega}$$
$$\times\sum_{N=0}^{\infty}\sum_{m_1=0}^{N}\sum_{m_2=0}^{\infty}\sum_{n_1=0}^{\infty}\sum_{n_2=0}^{N}\frac{(-1)^{m_1-n_2}e^{-\beta N\hbar\omega_c}N!(N-n_2+n_1)!(m_1+n_1)!\delta_{(n_1-n_2),(m_2-m_1)}}{m_1!m_2!n_1!n_2!(N-n_2)!(N-m_1)!}$$
$$\times\int_0^{\infty}\frac{dt}{t}[-1+(x+m_1+n_1+1)e^xE_{m_1+n_1+1}(x)](W_1+W_2+W_3)\ . \tag{4.8b}$$

In this expression,

$$W_1=-2D\left[t+\frac{\beta\hbar(n_1-n_2)\omega_c}{4t}\right], \tag{4.8c}$$

$$W_2=D\left[t+\frac{\beta\hbar(n_1-n_2)\omega_c+\omega}{4t}\right], \tag{4.8d}$$

$$W_3=D\left[t+\frac{\beta\hbar(n_1-n_2)\omega_c-\omega}{4t}\right]. \tag{4.8e}$$

Furthermore,

$$x=\frac{4t^2}{\beta\hbar\omega_c}+\frac{\hbar}{2m\omega_cL_D^2}\ , \tag{4.9}$$

and $n_I=\mathcal{N}/V$ is the ionized-impurity concentration. Note again that $\Xi^{(2)}_{\mathrm{imp},-}=\Xi^{(2)}_{\mathrm{imp},+}$. Therefore the simplified notation $\Xi^{(2)}_{\mathrm{imp},\perp}$ is introduced. The derivation of Eqs. (4.8) is analogous to the LO-phonon calculation in Sec. III, and the same notations are used. Again, it can be immediately seen that $\mathrm{Im}\Xi^{(2)}_{\mathrm{imp},\perp}$ is an even function of ω and $\mathrm{Re}\Xi^{(2)}_{\mathrm{imp},\perp}$ is an odd function of ω.

The theory will be compared with experiment at moderate temperatures ($T<75$ K in InSb). Therefore the expressions for $\Xi^{(2)}_{\mathrm{imp},\perp}$ can be simplified by only considering the terms dominant for $kT<\hbar\omega_c$ in Eqs. (4.8). This corresponds to neglecting the population of the higher Landau levels with $n>0$. Such a procedure results in a serious simplification: Only one summation remains, and we find

$$\mathrm{Im}\Xi^{(2)}_{\mathrm{imp},\perp}(\omega,\omega_c,kT<\hbar\omega_c)=\frac{n_I(2\pi\beta)^{1/2}e^4(1-e^{-\beta\hbar\omega_c})(1-e^{-\beta\hbar\omega})}{m^{1/2}\kappa^2\hbar\omega}$$
$$\times\sum_{l=0}^{\infty}e^{\beta(\hbar/2)(\omega-l\omega_c)}\int_0^{\infty}\frac{dt}{t}\exp\left[-t^2-\frac{\beta^2\hbar^2(|\omega|-l\omega_c)^2}{16t^2}\right][-1+(x+l+1)\exp(x)E_{l+1}(x)] \tag{4.10a}$$

and

$$\mathrm{Re}\Xi^{(2)}_{\mathrm{imp},\perp}(\omega,\omega_c,kT<\hbar\omega_c)=\frac{2n_I(2\beta)^{1/2}e^4(1-e^{-\beta\hbar\omega_c})}{m^{1/2}\kappa^2\hbar\omega}$$
$$\times\sum_{l=0}^{\infty}\int_0^{\infty}\frac{dt}{t}[-1+(x+l+1)\exp(x)E_{l+1}(x)]$$
$$\times\left[-2D\left[t+\frac{\beta\hbar l\omega_c}{4t}\right]+D\left[t+\frac{\beta\hbar(l\omega_c+\omega)}{4t}\right]+D\left[t+\frac{\beta\hbar(l\omega_c-\omega)}{4t}\right]\right]. \tag{4.10b}$$

The results of Eqs. (4.10) have been worked out numerically. In Fig. 2 typical plots of $\mathrm{Im}\Xi^{(2)}_{\mathrm{imp},\perp}$, $\mathrm{Re}\Xi^{(2)}_{\mathrm{imp},\perp}$, and $\mathrm{Re}(\sigma_{xx}+i\sigma_{xy})^{(2)}_{\mathrm{imp}}$ are shown, as a function of ω. The imaginary part of $\Xi^{(2)}_{\mathrm{imp},\perp}$ exhibits logarithmic divergences for $\omega=\pm l\omega_c$. Associated with these divergences, the real part shows finite jumps. Just as in the LO-phonon–scattering case, this behavior is a consequence of the inverse-square-root divergence from the integration of the product of two square-root divergences. For $\omega=0$ the $l=0$ term in Eq. (4.10a) leads to the well-known diver-

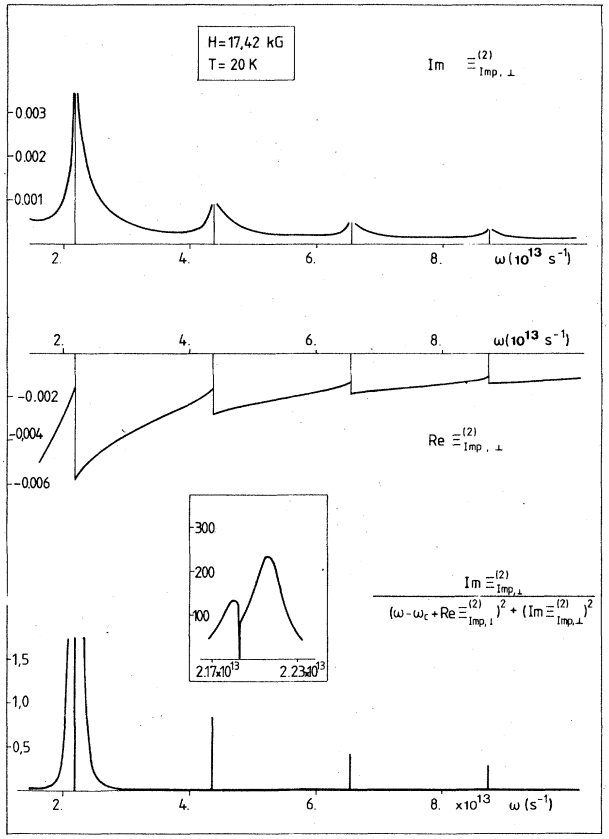

FIG. 2. Typical numerical results for the ionized-impurity-induced magneto-optical response functions in the Faraday configuration. The following parameters have been used (corresponding to InSb): magnetic field, $H=17.42$ kG; temperature, $T=20$ K; static dielectric constant, $\kappa=16.8$; parabolic band mass, $m=0.0139m_0$; ionized-impurity concentration, $n_I=5\times10^{14}$ cm^{-3}; free-carrier concentration, $n=1\times10^{14}$ cm^{-3}. The real and imaginary parts of the memory function $\Xi^{(2)}_{\text{imp},\perp}$ are calculated using Eqs. (4.10a) and (4.10b). The imaginary part of $\Xi^{(2)}_{\text{imp},\perp}$ shows logarithmic divergences at $\omega=n\omega_c$. The real part shows finite jumps at the same frequencies. The absorption spectrum in the active mode is calculated using Eq. (2.20). In the inset (lower panel) the structure of the calculated spectrum near $\omega=\omega_c$ is shown in full detail. The high-frequency maximum is considered to be the cyclotron-resonance line. It is broadened and shifted to higher frequencies (the divergence of $\text{Im}\Xi^{(2)}_{\text{imp},\perp}$ occurs exactly at the unperturbed cyclotron-resonance frequency). The lower structure on the left-hand side is considered to be spurious. It is due to the logarithmic divergence of $\text{Im}\Xi^{(2)}_{\text{imp},\perp}$ ($\omega=\omega_c$), in the lowest-order Born approximation. The divergences at $\omega=n\omega_c$ ($n=2,3,\ldots$) give rise to cyclotron-resonance harmonics. The response functions, which have dimension s, are given in units where $\omega_{\text{LO}}=1$.

gence of the dc resistivity in the lowest-order Born approximation. (An excellent review of the zero-frequency case has been given by R. Kubo, S. J. Miyake, and N. Hashitsuma in Ref. 54.) For $\omega=\omega_c$, a logarithmic divergence occurs due to the $l=0$ term. Since this singularity appears exactly at the position of the unperturbed cyclotron-resonance line, it is not immediately clear how a cyclotron-resonance linewidth can be extracted from the present calculation. In order to clarify this point, it is necessary to consider the inset of Fig. 2. Owing to the divergence of $\text{Im}\Xi^{(2)}_{\text{imp},\perp}$, the absorption coefficient shows a zero at $\omega=\omega_c$. From the figure it follows that the cyclotron-resonance peak is broadened and shifted away from the unperturbed frequency, to higher ω. At the low-frequency side the spectrum shows a shoulder which is spurious and due to the lowest-order Born approximation. The cyclotron-resonance linewidth can then be obtained from Fig. 2 by measuring the width at half maximum of the calculated peak. In Sec. V we will show that this interpretation leads to surprisingly good agreement with experimentally determined linewidths.

From the numerical results, it follows that a good approximation for the position of the calculated cyclotron-resonance peak is obtained by the equation

$$\omega-\omega_c+\text{Re}\Xi^{(2)}_{\text{imp},\perp}(\omega,\omega_c,T)=0\ , \tag{4.11}$$

and the linewidth is given by $\text{Im}\Xi^{(2)}_{\text{imp},\perp}(\omega,\omega_c,T)$ at the maximum of the cyclotron-resonance peak. Note that the lowest-order Born approximation predicts a negative shift of the cyclotron-resonance (CR) line, directly proportional to the ionized-impurity concentration.

For $l>1$ the divergences give rise to harmonics of cyclotron resonance.[49–52] These will be discussed in Sec. V.

It is interesting to consider how the present approach is different from previous methods. The calculation of Ref. 30 is essentially equivalent with the work of Kawabata.[2] In this paper the impurity-dominated cyclotron-resonance-linewidth calculation starts from the transport relaxation time τ_c for $\omega=\omega_c$. Such a procedure leads inevitably to a CR linewidth proportional to n_I. It is clear that such a calculation is essentially different from the present work, where the broadening *and* the shift of the CR line ($\omega\neq\omega_c$) are calculated explicitly.

V. COMPARISON WITH EXPERIMENT

A. Cyclotron-resonance linewidth in InSb: Temperature dependence

The cyclotron-resonance linewidth for free carriers in n-type InSb has been measured by Matsuda and Otsuka[29] in a temperature region from 4.2 up to 160 K. The experiment was carried out in the Faraday configuration, for different frequencies of the incident radiation. Various samples were investigated, with different concentrations of the ionized impurities and different free-carrier concentrations. For each sample the absorption coefficient was measured at constant radiation frequency and temperature T, as a function of magnetic field. The half width at half maximum of the cyclotron-resonance line was then determined. The experiment was repeated for different temperatures. In Figs. 3 and 4 the measured cyclotron-resonance linewidth is shown as a function of temperature for typical samples from Ref. 29. Essentially two regimes can be distinguished as a function of temperature. For $T<75$ K the half width varies rather slowly. In this regime, ionized-impurity scattering dominates. For $T\gtrsim75$ K the half width increases steeply. Here, optical-phonon scattering is important.

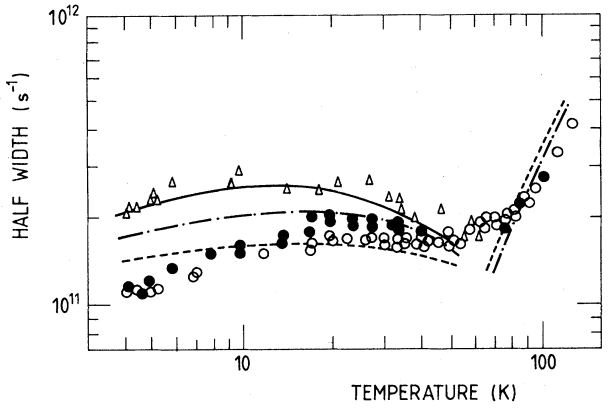

FIG. 3. Cyclotron-resonance half width in InSb as a function of temperature for different wavelengths of incident radiation. Open triangles, solid circles, and open circles denote experimental values obtained by Matsuda and Otsuka (Ref. 29) (172, 119, and 84 μm) for a sample with an ionized-impurity concentration of $n_I=5.5\times10^{14}$ cm^{-3} and a free-carrier concentration of $n=2.1\times10^{14}$ cm^{-3}. Solid, dashed-dotted, and dashed lines denote corresponding results of the present calculation. Low-temperature side, ionized-impurity scattering; high-temperature side, LO-phonon scattering.

The ionized-impurity-dominated regime is considered in more detail in Figs. 5–7. The half width as calculated with the present method is shown by the dashed lines. These results are obtained by numerically evaluating $\Xi^{(2)}_{\mathrm{imp},\perp}$ and $\Xi^{(2)}_{\mathrm{pol},\perp}$ [Eqs. (4.10) and (3.10), respectively], for a given frequency ω and temperature T, as a function of ω_c. Using Eq. (2.20) a plot is then made of $\mathrm{Re}(\sigma_{xx}+i\sigma_{xy})$ versus magnetic field. Since $\mathrm{Re}(\sigma_{xx}$

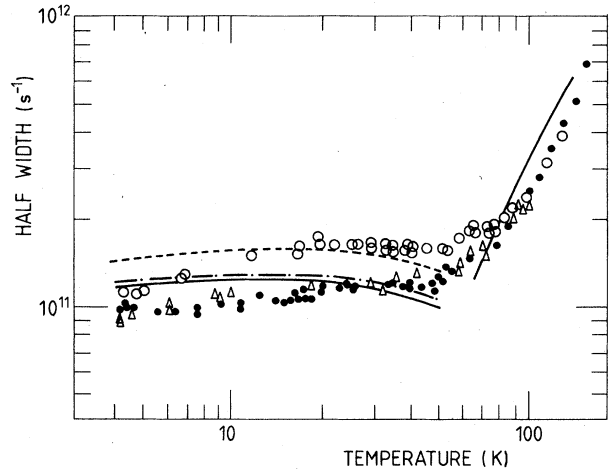

FIG. 4. Cyclotron-resonance half width in InSb as a function of temperature for different samples (84 μm). Sample parameters from experiment (Ref. 29) are as follows: Open circle, $n_I=5.5\times10^{14}$ cm^{-3} and $n=2.1\times10^{14}$ cm^{-3}; open triangle, $n_I=3.4\times10^{14}$ cm^{-3} and $n=0.81\times10^{14}$ cm^{-3}; solid circle, $n_I=3.6\times10^{14}$ cm^{-3} and $n=0.1\times10^{14}$ cm^{-3}. Dashed, solid, and dashed-dotted lines denote corresponding results of the present calculation. Low-temperature side, ionized-impurity scattering; high-temperature side, LO-phonon scattering. Obviously, the LO-phonon results are identical for the three samples.

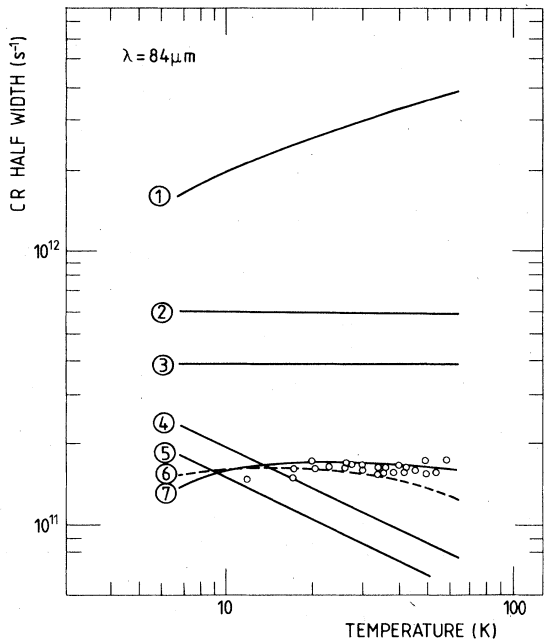

FIG. 5. Theoretical and experimental results for the cyclotron-resonance linewidth in InSb as a function of temperature. Open circles denote the experimental results of Matsuda and Otsuka (Ref. 29) for n-type InSb using incident radiation of wavelength $\lambda=84$ μm ($n_I=5.5\times10^{14}$ cm^{-3} and $n=2.1\times10^{14}$ cm^{-3}). 1, theoretical result of Shin *et al.* (Refs. 8 and 9). 2, theoretical result of Fujita and Lodder (Ref. 22). 3, theoretical result of Kawamura *et al.* (Ref. 1). 4, theoretical result of Arora and Spector (Ref. 30). 5, theoretical result of Kawabata (Ref. 2). 6, present calculation. 7, theoretical result of Bebenin (Ref. 17).

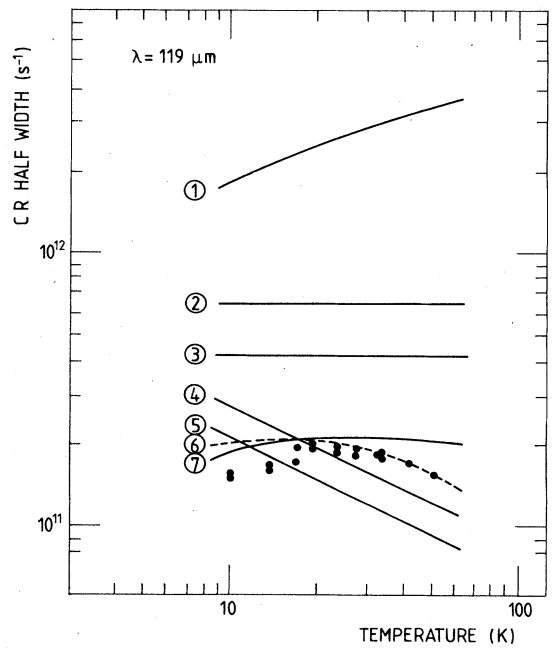

FIG. 6. Same as Fig, 5, but with a wavelength of incident radiation of $\lambda=119$ μm. The experimental results of Matsuda and Otsuka (Ref. 29) are indicated by solid circles.

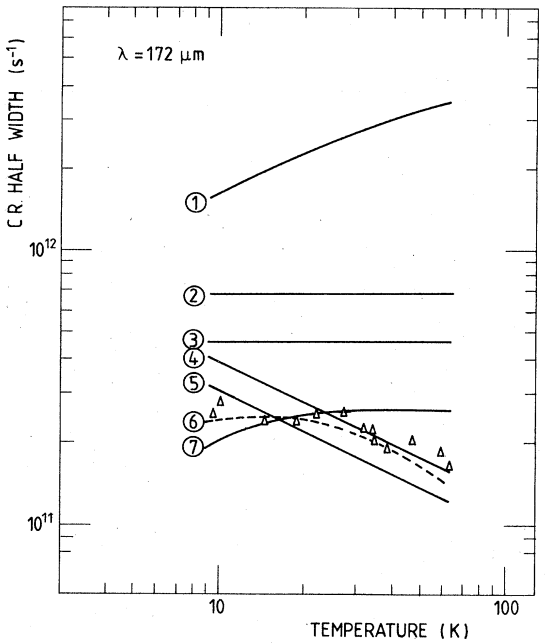

FIG. 7. Same as Fig. 5, but with a wavelength of incident radiation of $\lambda=172$ μm. The experimental results of Matsuda and Otsuka (Ref. 29) are indicated by open triangles.

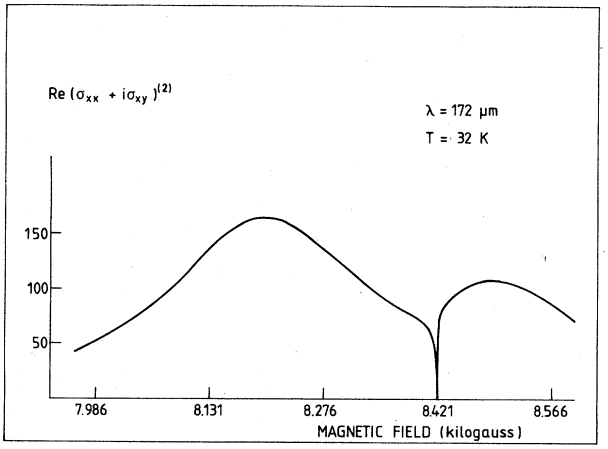

FIG. 8. Example of a theoretical spectrum used in the linewidth calculation (ionized-impurity scattering). The following parameters are used: temperature, $T=32$ K; wavelength of incident radiation, $\lambda=172$ μm; ionized-impurity concentration, $n_I=5.5\times10^{14}$ cm^{-3}; free-carrier concentration, $n=2.1\times10^{14}$ cm^{-3}; parabolic band mass, $m=0.0139m_0$; static dielectric constant, $\kappa=16.8$. Note the spurious structure due to the lowest-order Born approximation (cf. Fig. 2, where the spectrum is shown as a function of frequency of the incident radiation, at constant magnetic field).

$+i\sigma_{xy}$) is proportional to the optical-absorption coefficient, the theoretical half width of the cyclotron-resonance line can then be determined directly from the calculated spectrum. The following material constants have been used for InSb: parabolic band mass $m=0.0139m_0$,[50] static dielectric constant $\kappa=16.8$,[55] LO-phonon energy $\hbar\omega_{LO}=24.4$ meV,[50] and Fröhlich polaron coupling constant $\alpha=0.02$.[56] A typical example of a calculated spectrum used to obtain the linewidth is shown in Fig. 8.

From Figs. 3 and 4 it follows that good agreement is obtained between our calculation and experiment, in both regimes, for all wavelengths and samples under consideration.

For the sake of comparison we also show, in Figs. 5–7, the half widths as calculated in the impurity-scattering regime by other nonadjustable parameter theories, using a screened or unscreened Coulomb potential (solid lines). Note that the agreement with experiment for these theories is not very good, although in most cases quite sophisticated techniques have been used.

Special attention should be given to the low- and high-temperature limits of the impurity-scattering regime. For low temperatures ($T<15$ K) the agreement between our calculation and experiment is not so close. This is mainly due to the incomplete ionization of the impurities. The agreement could be easily improved by making the number of ionized impurities (and carriers) temperature dependent. A better description of the low-temperature region, however, would also necessitate the introduction of a different scattering potential: It is believed[38] that the anisotropy of the screening becomes important at low temperatures. The exact form of the potential, however, is not known. We will not consider corrections of this type here since the main purpose of the present paper is to investigate the relevance of the lowest-order Born approximation. Additional complications would only obscure our results.

As temperature is raised above 30 K, the experimental linewidth decreases slowly. Physically, this decrease can be easily understood in the framework of the present calculation. The width of the cyclotron-resonance line is mainly determined by $\mathrm{Im}\Xi^{(2)}_{\mathrm{imp},\perp}$ ($\omega\cong\omega_c$). Owing to the inverse-square-root divergence of the density of states in the z direction, the most important contribution to $\mathrm{Im}\Xi^{(2)}_{\mathrm{imp},\perp}$ ($\omega\cong\omega_c$) comes from carriers with small momentum along the direction of the magnetic field. As temperature increases, the number of low-p_z electrons decreases, and so does the linewidth. Note that the linewidth decrease is more pronounced for the larger-wavelength radiation, in agreement with the present calculation. It should also be noted that the experimental linewidth measured by Matsuda and Otsuka[29] is almost independent of the free-carrier concentration. This is illustrated in Fig. 4. Two samples are considered with comparable impurity concentration, but with free-carrier concentrations differing by a factor of $\cong8$. The calculated linewidths for these samples are almost identical, in agreement with experiment.

In the impurity-dominated regime, the cyclotron-resonance spectrum in InSb was observed earlier by McCombe *et al.*[20] For low temperatures the linewidth was found to be proportional to the square root of the ionized-impurity concentration. This result is in agreement with several theoretical calculations.[9,10,15] Recently, however, it has been argued that the $(n_I)^{1/2}$ behavior is a consequence of the competition of two independent mech-

anisms, namely ionized-impurity and acoustic-phonon scattering.[34] Therefore it is interesting to consider the result of the present, lowest-order calculation, taking into account only ionized-impurity scattering. In Fig. 9 the calculated linewidth is shown for InSb parameters as a function of ionized-impurity concentrations at $T=4.2$, 10, and 25 K (note the log-log scale). For comparison the slopes of n_I and $n_I^{1/2}$ are also indicated. Clearly, the present calculation yields a $(n_I)^{1/2}$ behavior at $T=4.2$ K, in agreement with the observations of McCombe *et al.*[20] At higher temperatures the exponent of n_I gradually increases to 1. This is in agreement with the measurements of Matsuda and Otsuka.[29] Indeed, for sufficiently high temperatures these authors observe a linewidth consistent with the effective inverse relaxation time obtained from zero-magnetic-field dc measurements. Obviously, in the impurity-dominated regime this result implies a linewidth proportional to n_I.

It is interesting to consider the low-temperature limit of the impurity-dominated cyclotron-resonance linewidth. In the work of McCombe *et al.*[20] a definite minimum was observed for this linewidth as a function of magnetic field. The present calculation, however, produces a linewidth decreasing monotonously with magnetic field. This discrepancy might be due to the use of a Debye-screened Coulomb potential in our calculation. As mentioned earlier, the introduction of an anisotropically screened potential is necessary at low temperatures. It has been shown by Heuser and Hajdu[21] that such a potential can produce a linewidth minimum.

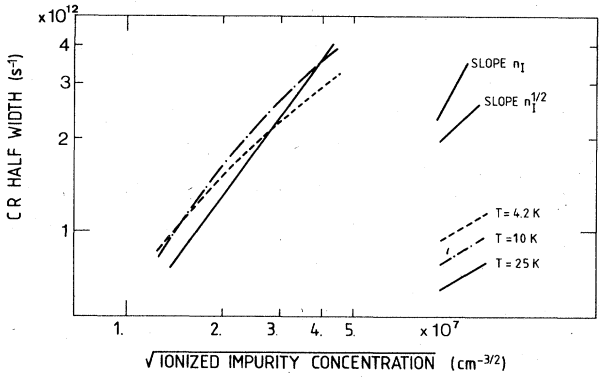

FIG. 9. Calculated cyclotron-resonance linewidth as a function of ionized-impurity concentration at different temperatures. InSb parameters are used for a sample with a free carrier concentration of $n=0.5\times10^{14}$ cm^{-3}. It is seen that the slope changes from an $n_I^{1/2}$ to an n_I behavior with increasing temperature. Note the logarithmic scale. For the sake of comparison, the slopes n_I and $n_I^{1/2}$ have been indicated.

B. Cyclotron-resonance harmonics and phonon-assisted harmonics

An interesting phenomenon observed in the magneto-optical conduction-band spectrum of InSb is the appearance of cyclotron-resonance harmonics and LO-phonon-assisted harmonics. These harmonics were first observed in samples with a free-carrier concentration of the order of 10^{16} cm^{-3}.[49–52] However, Grisar *et al.*[57] have improved the experimental resolution by using intraband photoconductivity. They have investigated samples with low free-carrier concentrations ($n=8\times10^{13}$ cm^{-3}). Various possible explanations have been given for the appearance of the cyclotron-resonance harmonics.[58–61] It was suggested by Mycielski *et al.*[60] that they are caused by ionized-impurity scattering ("impurity-assisted cyclotron resonance harmonics"). Owing to the low free-carrier concentration (nondegenerate limit) the results of our calculation can be compared immediately with the experiment of Grisar *et al.*[57] In the Voigt configuration, for $E\perp H$, the absorption coefficient is proportional to

$$\mathrm{Re}\sigma_{xx}=\tfrac{1}{2}[\mathrm{Re}(\sigma_{xx}+i\sigma_{xy})+\mathrm{Re}(\sigma_{xx}-i\sigma_{xy})]\ . \tag{5.1}$$

Starting from Eq. (2.20) and taking into account LO-phonon and ionized-impurity scattering, $\mathrm{Re}\sigma_{xx}$ can then be written as

$$\mathrm{Re}\sigma_{xx}=\frac{\frac{1}{2}(\mathrm{Im}\Xi^{(2)}_{\mathrm{pol},\perp}+\mathrm{Im}\Xi^{(2)}_{\mathrm{imp},\perp})}{(\omega-\omega_c+\mathrm{Re}\Xi^{(2)}_{\mathrm{pol},\perp}+\mathrm{Re}\Xi^{(2)}_{\mathrm{imp},\perp})^2+(\mathrm{Im}\Xi^{(2)}_{\mathrm{pol},\perp}+\mathrm{Im}\Xi^{(2)}_{\mathrm{imp},\perp})^2}$$
$$+\frac{\frac{1}{2}(\mathrm{Im}\Xi^{(2)}_{\mathrm{pol},\perp}+\mathrm{Im}\Xi^{(2)}_{\mathrm{imp},\perp})}{(\omega+\omega_c+\mathrm{Re}\Xi^{(2)}_{\mathrm{pol},\perp}+\mathrm{Re}\Xi^{(2)}_{\mathrm{imp},\perp})^2+(\mathrm{Im}\Xi^{(2)}_{\mathrm{pol},\perp}+\mathrm{Im}\Xi^{(2)}_{\mathrm{imp},\perp})^2}\ . \tag{5.2}$$

Here, $\Xi^{(2)}_{\mathrm{pol},\perp}$ and $\Xi^{(2)}_{\mathrm{imp},\perp}$ are given by Eqs. (3.10) and (4.10), respectively. From these analytical expressions it is immediately clear that LO-phonon-assisted and pure harmonics will indeed occur.

For comparison with the experiment of Grisar *et al.*,[57] an explicit numerical evaluation has been made of Eq. (5.2). (InSb parameters; $T=12$ K, $n=8\times10^{13}$ cm^{-3}, and $n_I=1\times10^{15}$ cm^{-3}.) The results are shown in Fig. 10. Obviously, the calculated intensity of the pure harmonics is at least 2 orders of magnitude smaller than the calculated intensity of the phonon-assisted harmonics. Moreover, note that the ionized-impurity concentration, $n_I=1\times10^{15}$ cm^{-3}, is certainly overestimated. Experimentally, the oscillator strengths of the two types of harmonics are found to be of comparable magnitude in photoconductivity measurements.[57] Although the photoconductivity is not directly proportional to the absorption coefficient, it is clear from our results that ionized-impurity scattering cannot possibly give rise to sufficiently strong cyclotron-resonance harmonics. We can conclude that the suggestion of Mycielski *et al.*[60] cannot explain the experimental observations in the present case. Note that this result is independent of the memory-function approach.

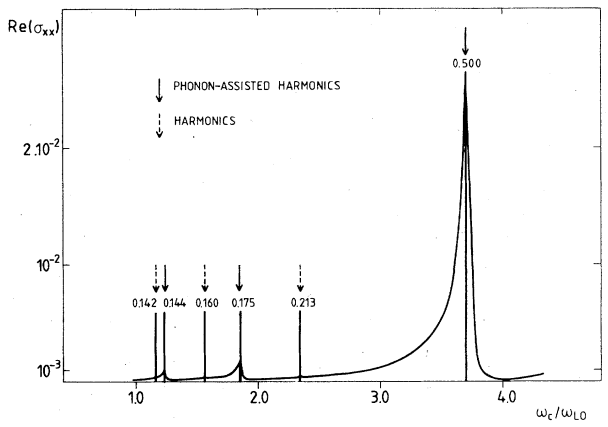

FIG. 10. Calculated cyclotron-resonance harmonics and phonon-assisted cyclotron-resonance harmonics using InSb parameters at $T=12$ K. Ionized-impurity concentration, $n_I=1\times10^{15}$ cm^{-3}; free-carrier concentration $n=8\times10^{13}$ cm^{-3}. The peak heights are indicated. The intensity of the harmonics is at least 2 orders of magnitude smaller than the intensity of the phonon-assisted harmonics.

VI. DISCUSSION AND CONCLUSIONS

The present paper was mainly motivated by the large discrepancies among various theoretical results for the quantum-limit cyclotron-resonance linewidth in semiconductors. As illustrated in Sec. IV, these results vary by more than an order of magnitude. Moreover, predictions are also qualitatively different and agreement with experiment is poor.

As far as elastic scattering is concerned, the problems are obviously related to the logarithmic divergence of the response functions at $\omega=\omega_c$ in the lowest-order Born approximation. Owing to this feature, any really satisfactory theory must be essentially nonperturbative. This seems to have been the major source of difficulties in most calculations: It has led to the introduction of various approximations, the validity of which is difficult to estimate. An important reason for the existence of several conflicting theories is the absence of a simple criterion to investigate the correctness of a linewidth calculation. The lowest-order Born approximation, however, is believed to yield good results for the spectrum, far from resonance. Therefore the present work can be useful as a test for more sophisticated calculations. Note that this argument is independent of the memory-function approach. It is difficult to judge theoretically the validity of the present method to obtain the linewidth. For ionized-impurity scattering, the calculated cyclotron-resonance peak is situated close to a (spurious) divergence, and this will certainly induce error. Note also that in the framework of many-body theory it has been shown by Miyake[31] that two distinct formulations of the lowest-order Born approximation lead to essentially different results. It is therefore rather surprising to see the close numerical fit in Figs. 3—7. Moreover, several qualitative predictions are also in agreement with experiment [the $(n_I)^{1/2}$ dependence of the linewidth at low temperatures, the linewidth decrease for $T>30$ K which is more pronounced for larger wavelength radiation, and the independence of the free-carrier concentration]. It will only be possible to understand this agreement, however, after performing a more sophisticated calculation in which the divergences are eliminated. In analogy with the dc case, such a calculation will have to incorporate collision broadening, inelasticity, and/or non-Born scattering.[54] Further improvements will also require the introduction of a more realistic model. This includes many-body effects, spin and umklapp processes, an anisotropically screened impurity potential, and most important, nonparabolicity (note that the experimental data presented in Figs. 3—7 have been treated by Matsuda and Otsuka[29] such as to eliminate the effects of nonparabolicity).

The present method can also be used to study the cyclotron-resonance linewidth measured in germanium by Kawamura *et al.*[1] in the regime dominated by ionized-impurity scattering. In this case, however, most experimental points are situated in the temperature region $kT>\hbar\omega_c$. Therefore, in the numerical calculations, the population of higher Landau levels must be taken into account, and the full expressions (4.8) must be evaluated [instead of Eqs. (4.10)]. This is left for future work. A recent calculation for these experimental data has only considered population of the lowest Landau levels.[35] It should be noted that in order to obtain good agreement with experiment it is essential to evaluate the lowest-order Born approximation in full detail. This is illustrated by the calculation of Ref. 17. The result of Ref. 17 can be obtained from our equations (4.10) by an (approximate) evaluation of the $l=1$ term only. This procedure leads to qualitative differences: The $(n_I)^{1/2}$ behavior for low temperatures is lost, and also, as can be seen from Figs. 5—7, the linewidth does not decrease for $T>30$ K.

As far as the electron-phonon interaction is concerned, it is interesting to consider the so-called "pinning region," for $\omega_c\cong\omega_{LO}$. In this special case, and for low temperatures, the present results are equivalent to those of earlier calculations.[6,23] These calculations were shown[6] to confirm Wigner-Brillouin perturbation theory, and they seemed to indicate a coupling constant $\alpha=0.03$—0.04 for InSb (also see Ref. 62). The present results, however, far from the pinning region, lead to the generally accepted value $\alpha=0.02$. This apparent contradiction is explained by a recent calculation[63] where it is shown variationally that Wigner-Brillouin perturbation theory does not give an adequate numerical description of the pinning region.

In conclusion, we have presented a calculation of the cyclotron-resonance spectrum for semiconductors in the quantum limit. No adjustable parameters have been introduced. Starting from the Kubo formula, we have shown that the lowest-order Born approximation leads to excellent agreement with measured cyclotron-resonance linewidths in InSb, both in the ionized-impurity- and LO-phonon-scattering regimes.

*Present address: Diamond High Council (H.R.D.), De Keyserlei 58-60, B-2018 Antwerpen, Belgium.

†Also at University of Antwerp (Universitair Instelling Antwerpen), Universiteitsplein 1, B-2610 Wilrijk, Belgium, and at Eindhoven University of Technology, 5600-MB Eindhoven, The Netherlands.

[1]H. Kawamura, H. Saji, M. Fukai, K. Sekido, and I. Imai, J. Phys. Soc. Jpn. **19**, 288 (1964).

[2]A. Kawabata, J. Phys. Soc. Jpn. **23**, 999 (1967).

[3]M. Saitoh and A. Kawabata, J. Phys. Soc. Jpn. **23**, 1006 (1967).

[4]S. J. Miyake, Phys. Rev. **170**, 726 (1968).

[5]C. J. Summers, R. B. Dennis, B. S. Wherrett, P. G. Harper, and S. D. Smith, Phys. Rev. **170**, 755 (1968).

[6]M. Nakayama, J. Phys. Soc. Jpn. **27**, 636 (1969).

[7]J. R. Apel, T. O. Poehler, C. R. Westgate, and R. I. Joseph, Phys. Rev. B **4**, 436 (1971).

[8]E. E. H. Shin, P. N. Argyres, and B. Lax, Phys. Rev. Lett. **28**, 1634 (1972).

[9]E. E. H. Shin, P. N. Argyres, and B. Lax, Phys. Rev. B **7**, 3572 (1973).

[10]E. E. H. Shin, P. N. Argyres, N. J. M. Horing, and B. Lax, Phys. Rev. B **7**, 5408 (1973).

[11]R. Kaplan, B. D. McCombe, and R. J. Wagner, Solid State Commun. **12**, 967 (1973).

[12]E. M. Gershenzon, N. A. Serebryakova, and V. B. Smirnova, Fiz. Tekh. Poluprovodn. **8**, 476 (1974) [Sov. Phys.—Semicond. **8**, 306 (1974)].

[13]E. M. Gershenzon, Yu. A. Gurvich, S. L. Orlova, and N. G. Ptitsina' Zh. Eksp. Teor. Fiz. **67**, 627 (1974) [Sov. Phys.—JETP **40**, 311 (1974)].

[14]P. N. Argyres, and J. L. Sigel, Phys. Rev. B **10**, 1139 (1974).

[15]A. Lodder and S. Fujita, Phys. Lett. **46A**, 381 (1974).

[16]A. Lodder, Solid State Commun. **16**, 117 (1975).

[17]N. G. Bebenin, Fiz. Tekh. Poluprovodn. **9**, 2114 (1975) [Sov. Phys.—Semicond. **9**, 1379 (1975)].

[18]E. Tyssen, R. Dornhaus, G. Haider, P. Kokoschinegg, K.-H. Müller, G. Nimtz, and H. Happ, Solid State Commun. **17**, 1459 (1975).

[19]R. Dornhaus, G. Nimtz, and E. Tyssen, Z. Phys. B **23**, 135 (1976).

[20]B. D. McCombe, R. Kaplan, R. J. Wagner, E. Gornik, and W. Müller, Phys. Rev. B **13**, 2536 (1976).

[21]M. Heuser and J. Hajdu, Solid State Commun. **20**, 313 (1976).

[22]S. Fujita and A. Lodder, Physica **83B**, 117 (1976).

[23]J. Van Royen, J. De Sitter, L. F. Lemmens, and J. T. Devreese, Physica **89B**, 101 (1977).

[24]G. M. Shmelev, I. A. Chaĭkovskiĭ, and Ch'ang K'uang Heng, Fiz. Tverd. Tela (Leningrad) **19**, 924 (1977) [Sov. Phys.—Solid State **19**, 538 (1977)].

[25]G. M. Shmelev, Fiz. Tverd. Tela (Leningrad) **20**, 3191 (1978) [Sov. Phys.—Solid State **20**, 1844 (1978)].

[26]R. Danzer and M. Kriechbaum, Acta Phys. Austriaca **49**, 27 (1978) (in German).

[27]W. Götze and P. Wölfle, Phys. Rev. B **6**, 1226 (1972); W. Götze and J. Hajdu, J. Phys. C **11**, 3993 (1978).

[28]J. P. Vigneron, R. Evrard, and E. Kartheuser, Phys. Rev. B **18**, 6930 (1978).

[29]O. Matsuda and F. Otsuka, J. Phys. Chem. Solids **40**, 809 (1979).

[30]V. K. Arora and H. N. Spector, Phys. Status Solidi B **94**, 701 (1979).

[31]S. J. Miyake, Prog. Theor. Phys. Suppl. **69**, 311 (1980).

[32]A. Suzuki, S. D. Choi, and S. Fujita, J. Phys. Chem. Solids **41**, 735 (1980).

[33]A. Bardasis and E. Yorke, Phys. Rev. B **23**, 4107 (1981).

[34]V. K. Arora, M. A. Al-Mass'ari, and M. Prasad, Phys. Rev. B **23**, 5619 (1981).

[35]T. K. Srinivas, S. Chaudhury, and S. Fujita, Solid State Commun. **37**, 919 (1981).

[36]R. J. Nicholas and C. K. Sarkar, Solid State Commun. **41**, 943 (1982).

[37]P. N. Argyres and E. N. Adams, Phys. Rev. **104**, 900 (1956).

[38]N. J. Horing, Ann. Phys. (N.Y.) **54**, 405 (1969).

[39]R. Kubo, J. Phys. Soc. Jpn. **12**, 570 (1957).

[40]J. Van Royen and J. T. Devreese, Solid State Commun. **40**, 947 (1981).

[41]D. M. Larsen, Phys. Rev. **135**, A419 (1964).

[42]J. Callaway, *Quantum Theory of the Solid State* (Academic, New York, 1974), Pt. B, p. 528.

[43]J. Devreese, W. Huybrechts, and L. Lemmens, Phys. Status Solidi B **48**, 77 (1971).

[44]J. T. Devreese, J. De Sitter, and M. Goovaerts, Phys. Rev. B **5**, 2367 (1971); R. P. Feynman, R. Hellwarth, C. Iddings, and P. Platzman, *ibid.* **127**, 1004 (1962).

[45]*Polarons and Excitons,* edited by C. Kuper and G. Whitfield (Oliver and Boyd, Edinburgh, 1963).

[46]*Polarons in Ionic Crystals and Polar Semiconductors,* edited by J. T. Devreese (North-Holland, Amsterdam, 1972).

[47]I. S. Gradshteyn and I. M. Ryzhik, *Table of Integrals, Series and Products* (Academic, New York, 1965).

[48]*Handbook of Mathematical Functions,* edited by M. Abramowitz and I. A. Stegun (Dover, New York, 1964).

[49]R. C. Enck, A. S. Saleh, and H. Y. Fan, Phys. Rev. **182**, 790 (1969).

[50]E. J. Johnson and D. H. Dickey, Phys. Rev. B **1**, 2676 (1970).

[51]M. H. Weiler, R. L. Aggarwal, and B. Lax, Solid State Commun. **14**, 299 (1974).

[52]G. Favrot, R. L. Aggarwal, and B. Lax, Solid State Commun. **18**, 577 (1976).

[53]Y. Ono and J. Hajdu, Z. Phys. B **33**, 61 (1979).

[54]R. Kubo, S. J. Miyake, and N. Hashitsume, *Quantum Theory of Galvanomagnetic Effect at Extremely Strong Magnetic Fields,* Vol. 17 of *Solid State Physics,* edited by F. Seitz and D. Turnbull (Academic, New York, 1965), p. 269.

[55]E. Kartheuser, in *Polarons in Ionic Crystals and Polar Semiconductors,* Ref. 46, p. 726.

[56]J. R. Dixon and J. K. Furdyna, Solid State Commun. **35**, 195 (1980).

[57]R. Grisar, H. Wachernig, G. Bauer, J. Własak, J. Kowalski, and W. Zawadzki, Phys. Rev. B **18**, 4355 (1978).

[58]B. D. McCombe, R. J. Wagner, S. Teitler, and J. J. Quinn, Phys. Rev. Lett. **28**, 37 (1972).

[59]S. J. Miyake, J. Phys. Soc. Jpn. **35**, 551 (1973).

[60]J. Mycielski, G. Bastard, and C. Rigaux, Phys. Rev. B **16**, 1675 (1977).

[61]M. H. Weiler, R. L. Aggarwal, and B. Lax, Phys. Rev. B **17**, 3269 (1978).

[62]E. S. Koteles and W. R. Datars, Phys. Rev. B **14**, 1571 (1976).

[63]G. Lindemann, R. Lassnig, W. Seidenbusch, and E. Gornik, Phys. Rev. B **28**, 4693 (1983).